AIP Advances

Across-plane thermal characterization of films based on amplitude-frequency profile in photothermal technique

Shen Xu and Xinwei Wang

Citation: AIP Advances **4**, 107122 (2014); doi: 10.1063/1.4898330
View online: http://dx.doi.org/10.1063/1.4898330
View Table of Contents: http://scitation.aip.org/content/aip/journal/adva/4/10?ver=pdfcov
Published by the AIP Publishing

Across-plane thermal characterization of films based on amplitude-frequency profile in photothermal technique

Shen Xu and Xinwei Wang[a]
Department of Mechanical Engineering, Iowa State University, Ames, Iowa 50011, USA

(Received 30 May 2014; accepted 1 October 2014; published online 13 October 2014)

This work develops an amplitude method for the photothermal (PT) technique to analyze the amplitude of the thermal radiation signal from the surface of a multi-layered film sample. The thermal conductivity of any individual layer in the sample can be thereby determined. Chemical vapor deposited SiC film samples (sample 1 to 3: 2.5 to 3.5 μm thickness) with different ratios of Si to C and thermally oxidized SiO_2 film (500 nm thickness) on silicon substrates are studied using the amplitude method. The determined thermal conductivity based on the amplitude method is 3.58, 3.59, and 2.59 W/m·K for sample 1 to 3 with ±10% uncertainty. These results are verified by the phase shift method, and sound agreement is obtained. The measured thermal conductivity (k) of SiC is much lower than the value of bulk SiC. The large k reduction is caused by the structure difference revealed by Raman spectroscopy. For the SiO_2 film, the thermal conductivity is measured to be 1.68±0.17 W/m·K, a little higher than that obtained by the phase shift method: 1.31±0.06 W/m·K. Sensitivity analysis of thermal conductivity and interfacial resistance is conducted for the amplitude method. Its weak-sensitivity to the thermal contact resistance, enables the amplitude method to determine the thermal conductivity of a film sample with little effect from the interface thermal resistance between the film and substrate. The normalized amplitude ratio at a high frequency to that at a low frequency provides a reliable way to evaluate the effusivity ratio of the film to that of the substrate. [http://dx.doi.org/10.1063/1.4898330]

I. INTRODUCTION

Film materials play a basic role in today's industry, so knowing properties of films along their cross-sectional direction becomes more important in the thermal design of a device. Many techniques have been developed over past decades to measure the thermophysical properties of thin films. One important class of those techniques is the 3ω method.[1–3] This technique utilizes a microfabricated metal line deposited on the specimen to act as a resistive heater. An AC current is fed through the metal line with a frequency of ω. The periodic heating generates a temperature variation and oscillations in the electrical resistance at the second harmonic frequency, thus leading to a 3ω variation in the voltage. The resulting amplitude and phase shift of this third harmonic voltage signal are then used to characterize thermophysical properties. The 3ω method gives a relatively better signal-to-noise ratio. The I-V behavior and the temperature coefficient of the resistance of the sample film need to be known or calibrated separately.

Another class of techniques employs optical and noncontact measurements, known as the pump-probe technique, to study thin film's properties. A feature of the pump-probe technique is the use of ultrafast lasers to measure transient events on picoseconds time. The technique has been widely applied in diverse fields such as ultrafast spectroscopy,[4,5] photo-acoustics,[6,7] Terahertz imaging,[8] and etc. For the transient thermoreflectance (TTR) technique,[9] it is a pump-probe type of measurement. Two ultrafast laser pulses of a few picoseconds pulse width or shorter irradiate

[a]Corresponding author. Email: xwang3@iastate.edu. Phone: 515-294-2085. Fax: 515-294-3261.

the sample surface. The first pulse heats the sample and leads to the reflectance change of the sample surface, while the second pulse is weaker and slightly delayed to probe this reflectance variation. The resulting change in the reflectivity is linearly proportional to the temperature change within a small temperature range.[10,11] Determining the thermal diffusivity of thin films, the TTR technique using ultrashort pulsed lasers has been demonstrated as an effective tool for measuring the thermophysical and mechanical properties of thin materials.

The photoacoustic (PA) technique relates acoustic signals to the incident light for thermophysical property measurements. Rosencwaig and Gersho[12] first developed the RG model to understand the PA phenomenon. Since then, many works based on this model have been carried out and focused on thermal transport in multilayer samples.[13–16] Generally, a modulated laser is focused on the sample surface to generate local heating. The sample surface temperature variation is then detected by measuring small pressure variations in the gas adjacent to the surface.[17]

The photothermal (PT) technique[18–20] that has been used in our lab is also based on the PA principle. It improves the PA technique by measuring the radiation variation from a sample's surface instead of the measurement of acoustic signals. In the PT technique for thermal characterization, the phase shift between the measured thermal response and the laser is frequently used. The phase shift variation is sensitive to the thermal conductivity along the thickness direction and interfacial resistances. The pulsed laser-assisted thermal relaxation (PLTR) technique[21,22] can be treated as an extension of the PT technique, which was also developed in our lab to measure the thermophysical properties of one-dimensional structures. Photon heating is used as a heat source and the voltage variation over a filament is used for thermal probing. It is a transient technology for characterizing the thermal diffusivity along the axial direction of micro/nanoscale structures. The PLTR2 technique[23] is a further improvement on the PLTR technique, and can simultaneously measure thermal properties of free-standing films along both in-plane and thickness directions.

In this work, the PT technique is further developed to use the amplitude of thermal radiation to determine the thermophysical properties of films in the thickness direction. Amplitude has rarely been used in previous work because of its complexity. The absolute amplitude of thermal radiation is determined by many factors, like the sample's surface reflection, absorption, emissivity, the experimental setup, and the sensitivity of the infrared detector. Instead of its absolute value, the shape of reduced amplitude against the modulation frequency is used for thermophysical properties determination in our work. SiC films of 2~3 μm thickness on Si are characterized and compared with the results from the phase shift method. The sensitivity of this amplitude technique is studied in detail, and its accuracy is examined by comparing the results with that of those determined using phase shift fitting.

II. PHYSICS OF THE METHOD

The PT technique[18–20] was developed for studying thermal transport across a multilayer film model. A modulated laser beam is applied to the surface of the material as a heat source, causing the radiation signal from the sample's surface to contain information about thermoproperties of layers beneath the top layer. Considering that the thermal diffusion length in the gas and the target layer is much smaller than the diameter of the laser beam when the laser focal spot is large enough, the PT experiment can be simplified as a one-dimensional cross-plane heat transfer model for describing temperature distribution and evolution. The cross-sectional view of the multilayer model is shown in Fig. 1(a). Layers from 1 to N are sample layers between the substrate (layer 0) and the gas layer (layer N + 1). The incident laser is a square-wave modulated monochromatic laser beam with a modulation frequency f. Layer i thereby has a thickness of $L_i = l_i - l_{i-1}$. Other thermophysical properties of the layer i are noted as: thermal conductivity k_i, specific heat $c_{p,i}$, thermal diffusivity α_i, and optical absorption coefficient β_i. Other parameters needed in the physical model are the thermal diffusion length $\mu_i = \sqrt{\alpha_i/\pi f}$, thermal diffusion coefficient $a_i = 1/\mu_i$, and thermal contact resistance between layer i and $(i + 1)$, $R_{i,i+1}$. Therefore, the governing equation for a multilayer 1D thermal diffusion problem in layer i can be expressed as

$$\frac{\partial^2\theta_i}{\partial x^2} = \frac{1}{\alpha_i}\frac{\partial\theta_i}{\partial t} - \frac{\beta_i I_0}{2k_i}\exp\Big(\sum_{m=i+1}^{N} -\beta_m \mathrm{L}_m\Big) \times \mathrm{e}^{\beta_i(\mathrm{x}-l_i)}(1 + e^{j\omega t}) \quad (1)$$

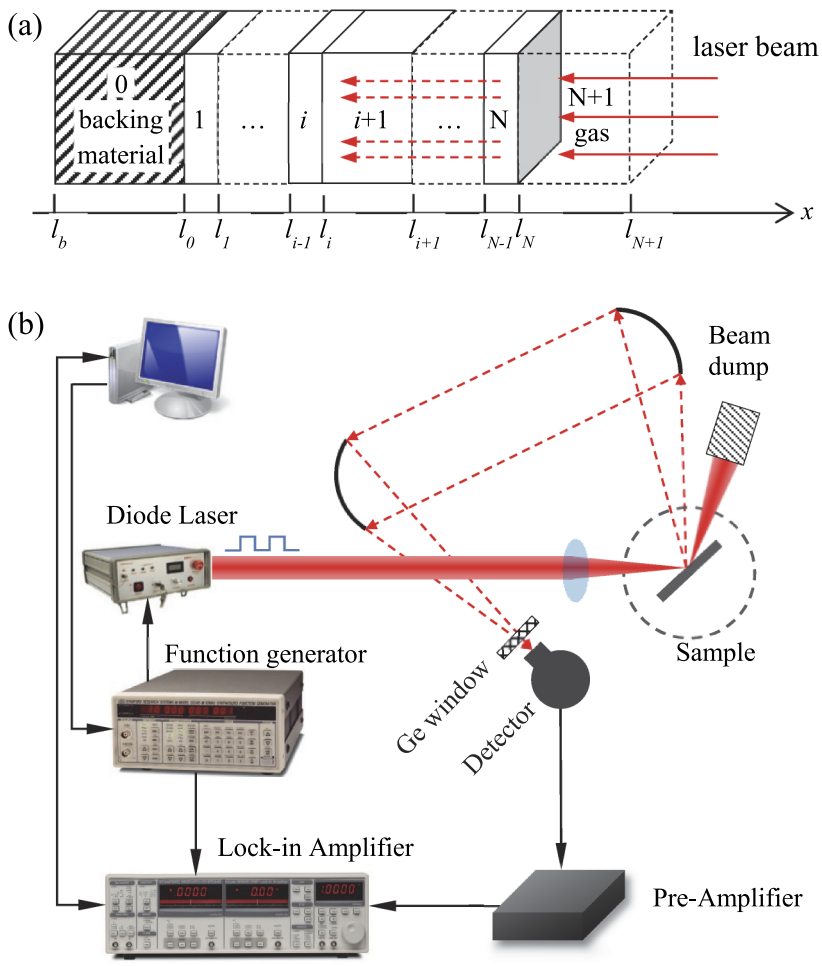

FIG. 1. (a) Schematic of an N-layer sample. It shows the multiple layers model. The x axis is along the thickness direction of the model. (b) The experimental setup of the PT technique.

where $\theta_i = T_i - T_{amb}$ is the modified temperature of layer i, and T_{amb} is the ambient temperature. ω is the angular frequency $(2\pi f)$. The solution θ_i to Eq. (1) is composed of the transient component $\theta_{i,t}$, the steady DC component $\overline{\theta}_{i,s}$ and the steady AC component $\widetilde{\theta}_{i,s}$. Among the previous three terms, only the AC component $\widetilde{\theta}_{i,s}$ will be collected for further evaluation and data processing. The general solution of $\widetilde{\theta}_{i,s}$ can be expressed as following equation:

$$\widetilde{\theta}_{i,s} = [\mathrm{A}_i e^{\sigma_i(\mathrm{x}-l_i)} + \mathrm{B}_i e^{-\sigma_i(\mathrm{x}-l_i)} - \mathrm{E}_i e^{\beta_i(\mathrm{x}-l_i)}]e^{j\omega t} \tag{2}$$

where $E_i = G_i/(\beta_i^2 - \sigma_i^2)$ with $G_i = \frac{\beta_i I_0}{2k_i} \exp(-\sum_{m=i+1}^{N} \beta_m \mathrm{L}_m)$, and for $i < N$, $G_N = \beta_N I_0/2k_N$, and $G_{N+1} = 0$. σ_i is defined as $(1 + j)\cdot a_i$ with $j = \sqrt{-1}$.

To obtain coefficients A_i and B_i, both the gas layer and backing material are assumed to be thermally thick (sufficiently met in the experiment), so that $A_{N+1} = 0$ and $B_0 = 0$. The rest of coefficients are determined by using the interfacial conditions at $x = l_i$, as

$$\begin{bmatrix} A_i \\ B_i \end{bmatrix} = U_i \begin{bmatrix} A_{i+1} \\ B_{i+1} \end{bmatrix} + V_i \begin{bmatrix} E_i \\ E_{i+1} \end{bmatrix} \tag{3}$$

where U_i is the interfacial transmission matrix of heat and V_i is the absorption matrix of light from layer $i + 1$ to i.[24] They are expressed as

$$U_i = \frac{1}{2}\begin{bmatrix} u_{11,i} & u_{12,i} \\ u_{21,i} & u_{22,i} \end{bmatrix}; V_i = \frac{1}{2}\begin{bmatrix} v_{11,i} & v_{12,i} \\ v_{21,i} & v_{22,i} \end{bmatrix}, \tag{4}$$

$$\text{where } u_{1n,i} = (1 \pm k_{i+1}\sigma_{i+1}/k_i\sigma_i \mp k_{i+1}\sigma_{i+1}R_{i,i+1}) \times \exp\left[\mp\sigma_{i+1}(l_{i+1} - l_i)\right], n = 1,2, \tag{4a}$$

$$u_{2n,i} = (1 \mp k_{i+1}\sigma_{i+1}/k_i\sigma_i \mp k_{i+1}\sigma_{i+1}R_{i,i+1}) \times \exp\left[\mp\sigma_{i+1}(l_{i+1} - l_i)\right], n = 1,2, \tag{4b}$$

$$v_{n1,i} = 1 \mp \beta_i/\sigma_i, n = 1,2, \tag{4c}$$

$$\text{and } v_{2n,i} = (-1 \mp k_{i+1}\beta_{i+1}/k_i\sigma_i \mp k_{i+1}\beta_{i+1}R_{i,i+1}) \times \exp\left[-\beta_{i+1}(l_{i+1} - l_i)\right], n = 1,2. \tag{4d}$$

Thus, the coefficients A_i and B_i are obtained using

$$B_{N+1} = -\frac{\begin{bmatrix} 0 & 1 \end{bmatrix} \sum_{m=0}^{N} (\prod_{i=0}^{m-1} U_i) V_m \begin{bmatrix} E_m \\ E_{m+1} \end{bmatrix}}{\begin{bmatrix} 0 & 1 \end{bmatrix} (\prod_{i=0}^{m-1} U_i) \begin{bmatrix} 0 \\ 1 \end{bmatrix}} \tag{5a}$$

$$\begin{bmatrix} A_i \\ B_i \end{bmatrix} = (\prod_{m=i}^{N} U_m) \begin{bmatrix} 0 \\ B_{N+1} \end{bmatrix} + \sum_{m=i}^{N} (\prod_{k=i}^{m-1} U_k) V_m \begin{bmatrix} E_m \\ E_{m+1} \end{bmatrix} \tag{5b}$$

The PT signal can be expressed in terms of surface temperature T of the top layer, and the measured radiation variation is proportional to the surface temperature change. Detailed calculations are provided in Ref. 17. These equations are listed here for further discussion of physical meanings and sensitivity in our amplitude method.

In previous studies with the PT technique, the amplitude data was not used to determine a film's properties due to the fact that the absolute amplitude (raw data, A_{raw}) is affected by many factors other than the rise in temperature, such as the experimental setup (optical alignment), the sample's surface properties, and the sensitivity of the infrared detector. An amplitude normalizing procedure is thus introduced to process A_{raw} before it is used for fitting.

The experimental system will inevitably produce systematic uncertainty and energy loss, so amplitude variations of the incident laser will also affect radiation signals. The sample's surface properties should also be considered, like surface emissivity and absorptivity. Calibration data is required before the PT measurement to exclude the effect of the incident laser amplitude variation against frequency. The influence of other parameters can be grouped in a universal constant during data fitting discussed later. A metal coated substrate with a large thermal conductivity is used during calibration. With the reflected laser amplitude (A_{cal}) from this metallic surface, the laser output variation effect can be eliminated by dividing A_{raw} by A_{cal}.

Furthermore, the frequency f also affects the raw amplitude by modulating the incident laser during the entire PT experiment. The measured amplitude decreases quickly as the frequency increases since the heating time is shorter in each period in the higher frequency range. The sensitivity is also lower in the higher frequency range, so the modulation effect should be considered. The total energy input amount depends on the irradiation time and the incident intensity. For physical analysis, when the modulated laser irradiates the metallic film, the total incident energy arriving at the sample surface (ΔE) in one heating period is $\Delta E = 0.5\varepsilon I_0/f$, where I_0 is the laser intensity, and ε the surface absorptivity. I_0 is proportional to the reflected laser amplitude A_{cal}. For the modulation frequency, the longer the laser irradiates $(1/f)$, the higher the temperature rises on the metallic surface. Another relevant parameter, the thermal diffusion length $\mu = \sqrt{\alpha/\pi f}$, depends on both the thermal diffusivity α and the frequency f. A higher frequency will shorten the diffusion length and concentrate the absorbed energy into a smaller depth. Amplitude A_{raw} is the combination of these two factors as

$$\frac{A_{raw}}{A_{cal}} \sim \frac{\zeta/f}{\sqrt{\alpha/f} \cdot \rho c_p} = \frac{1}{\sqrt{f}} \cdot \frac{\zeta}{\sqrt{k\rho c_p}}, \tag{6}$$

where ζ is a coefficient related to ε and other factors in the experiment, including detector sensitivity, surface emissivity, and collection angle of the paralloidal mirrors. ζ is a constant across all the

frequencies. f is the only changing variable in Eq. (6). Therefore, the processed result A_{raw}/A_{cal} is further normalized by multiplying $\sqrt{f}$ to get rid of the frequency effect. The normalized amplitude A_{nor}, can be expressed as

$$A_{nor} = \frac{A_{raw} \cdot \sqrt{f}}{A_{cal}} \sim \frac{\zeta}{\sqrt{k\rho c_p}} = \frac{\zeta}{e} \tag{7}$$

where e is the effusivity of the sample with the expression $e = \sqrt{k\rho c_p}$. The physical meaning of thermal effusivity is the thermal energy needed for 1 K temperature rise in the characteristic thermal diffusion length per unit area per second. Equation (7) shows that A_{nor} is inversely proportional to e of the sample, including the sample layer and the substrate.

After obtaining the normalized amplitude, the fitting program is run to fit the shape of the normalized amplitude against frequency. During this process, we first use guessed initial values of thermal conductivity and specific heat for the layer of interest. The program will then start calculating the theoretical amplitude curve against the frequency and compare it with the A_{nor} curve using the least square method. A universal constant C groups all other parameters mentioned above containing effects of the surface reflectivity, absorptivity, infrared detector sensitivity and radiation collection angle by the paraballoidal mirrors. When processing the data, the normalized theoretical amplitude $A_{nor,the}$ is multiplied by C and then compared with the normalized experiment amplitude $A_{nor,exp}$ at each frequency, $(A_{nor,exp} - C{\cdot}A_{nor,the})_f$. For guessed values of thermophysical properties, the constant C is determined as follows. The sum of the square of this term $[(A_{nor,exp} - C{\cdot}A_{nor,the})_f]$ at all frequencies should be the minimum value. Thus, the derivative should be 0 and C can be determined using $\sum_f A_{nor,exp,i} \cdot A_{nor,the,i} / \sum_f A^2_{nor,the,i}$. The thermal conductivity and specific heat are then adjusted until finding the best theoretical curve that fits the shape of the experimental curve. The final thermal conductivity and specific heat are taken as the properties of the layer of interest.

III. ACROSS-PLANE THERMAL CHARACTERIZATION OF SiC AND SiO_2 FILMS ON Si

A. Sample and experiment details

In this work, we measure SiC films grown on Si to demonstrate the capacity of the amplitude method and compare the results with the phase shift method which has been used and verified extensively in the past. The chemical vapor deposited (CVD) SiC samples on the Si substrate are from Veeco with a size of 1"x 1". Two different ratios of Si and C are used in their film growth: 50% Si / 50% C for sample 1 and 2, and 20% Si / 80% C for sample 3. An 80 nm-thick Cr film is sputter coated on top of the SiC to absorb the laser beam and generate heat in experiment. The very fine thickness (80 nm) of the Cr coating has very little effect on the measurement result.

For the PT technique, both the principle and the experimental setup of the measurement are shown in Fig. 1. A continuous infrared diode laser (809 nm) is modulated by a function generator and focused on the sample surface with a convex lens. The metallic layer on top of the sample absorbs the periodic energy from the modulated laser and generates heat as a heating source. A periodic temperature variation on the surface arises which causes a variation in the thermal emission from the sample surface. The thermal emission is collected by two off-axis paraboloidal mirrors and then collected and identified by an infrared detector (J15D12-M204-S01M-60, Jusdon Technologies). In front of the detector, a Ge window filters out the reflected laser beam from the sample and only allows the thermal radiation to pass. The thermal radiation is converted into electrical signals, pre-amplified and then sent to a lock-in amplifier. The whole experiment is controlled by a program for automatic data acquisition and noise suppression. The experimental frequency range is 400 Hz to 20 kHz.

B. The phase shift method

To evaluate the accuracy of the amplitude method, the phase shift method is conducted first to determine the sample's thermal conductivity and interface resistance for comparison. In our fitting,

the properties of the air layer, the metal coating, the sample layer, and the substrate are taken from references:[25] For samples 1, 2, and 3, the 80 nm thick Cr film has a thermal conductivity k of 93.7 W/m·K, a specific heat c_p of 449 J/kg·K, and density ρ of 7160 kg/m^3. The Si substrate has a thermal conductivity k of 148 W/m·K, the specific heat c_p of 712 J/kg·K, and the density ρ of 2330 kg/m^3. The bulk density and specific heat of SiC, 690 J/kg·K and 3160 kg/m^3, are used here because these two properties for the CVD SiC are weakly determined by the structure. They should have little deviation from the bulk's values.

For PT signals, the phase shift of the thermal radiation has been used broadly and extensively in our group. Its accuracy and reliability are well documented.[18–20] The fitted result for sample 1 using the phase shift method is plotted in Fig. 2(a). Sound agreement is observed between the fitting result and the experimental data. The final thermal conductivity is fitted as 3.72 W/m·K and the thermal contact resistance $R''_{\mathrm{Si,SiC}}$ is determined to be 1.5×10^{-7} m^2·K/W. The experimental statistical uncertainty (the blue hollow squares in Fig. 2(a)) is calculated using $\sqrt{\xi^2_{\phi_{raw}} + \xi^2_{\phi_{cal}}}$, where $\xi_{\phi_{raw}}$ and $\xi_{\phi_{cal}}$ are statistical uncertainty of the phase shift for the raw data and calibration data, respectively. Both $\xi_{\phi_{raw}}$ and $\xi_{\phi_{cal}}$ are acquired during the PT measurement and calibration. For the fitting uncertainty of thermal conductivity, the theoretical curves with k of 3.42 W/m·K and 4.02 W/m·K show obvious deviation from the best fitting result. In fact, the deviation is much larger than the experimental uncertainty of the phase shift. Therefore, we can conclude the fitting uncertainty of the thermal conductivity is ±8%.

C. The amplitude method

For the amplitude method, the raw amplitude of radiation signal A_{raw} and the reflected laser intensity (the calibration amplitude) A_{cal} for sample 1 are shown in Fig. 2(b). The statistical uncertainty $\xi_{A_{raw}}$ is collected while the raw amplitude is being acquired during the measurement. A_{raw} decreases quickly as the frequency increases. For all samples, the raw amplitude has the same trend and shape against the frequency so that the differences in heat transfer for different samples are difficult to distinguish from the raw amplitude. This significantly illustrates the fact that the effect of f lowers the sensitivity of A_{raw}. By multiplying A_{raw} by $\sqrt{f}$ in the normalization, we can easily extract the difference in heat transfer for each sample over the entire frequency range and thereby fit the variation of the amplitude and obtain its thermophysical properties. The reflected intensity of the laser A_{cal} (black dots in the inset plot of Fig. 2(b)) is very steady with only 4.8% variation across the whole measurement. It is affected by the modulation frequency to a very limited extent. The tiny change of the irradiation laser is also considered in our amplitude fitting as described above. Its statistical uncertainty $\xi_{A_{cal}}$ in the inset plot is much lower, about 0.1% of A_{cal}, indicating the sound steadiness of the laser source.

After excluding influences from the systematic noise, experimental setup and frequency, the final normalized amplitude A_{nor} (black dots in Fig. 2(c)) for sample 1 gradually increase relative to the frequency from 0.3 to 1. A_{nor} at a higher frequency becomes more significant for determining the shape of the change of the A_{nor} curve and thereby fitting k. Opposite to the raw data, A_{nor} becomes more sensitive. Its small variation can be easily detected especially in the high frequency range due to the fact that the modulation effect is removed. With the same parameters used in the phase shift method, a thermal conductivity k of 3.58 W/m·K is obtained based on amplitude fitting. Also the curves with k = 3.23 W/m·K and k = 3.94 W/m·K clearly show ±10% deviation of the thermal conductivity. The experimental statistical uncertainty $\xi_{A_{nor}}$ is calculated using $|A_{nor}| \times \sqrt{\left(\frac{\xi_{A_{raw}}}{A_{raw}}\right)^2 + \left(\frac{\xi_{A_{cal}}}{A_{cal}}\right)^2}$. Its value is about five orders of magnitude less than A_{nor} which is much smaller than ±10%. Therefore, the fitting uncertainty of the thermal conductivity for the amplitude method is determined to be ±10%.

Thermal conductivity fitted with both the phase shift and the amplitude methods for all SiC/Si samples are listed in the Table I. The amplitude method gives very close fitting results of thermal conductivity to the phase shift method. The deviations between these two methods are 4%, 7%, and 16% for samples 1, 2, and 3, respectively. However, the thermal contact resistance is hard to be determined

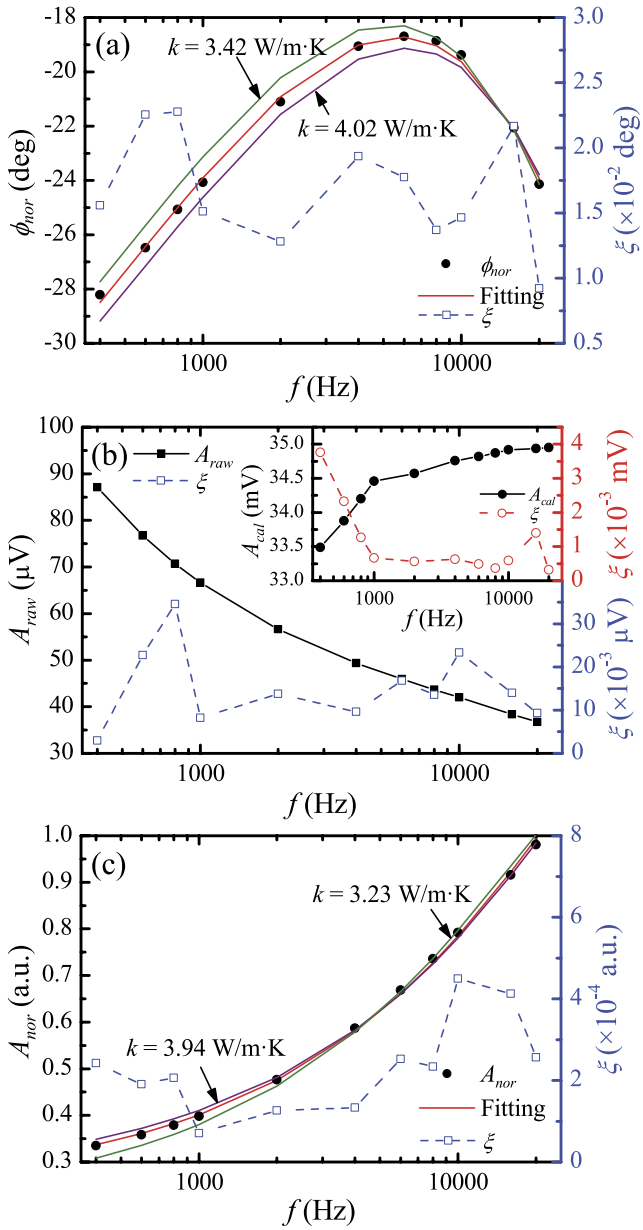

FIG. 2. (a) The fitting result based on the phase shift method for the 2.5 μm SiC film on Si. The thermal conductivity is determined at 3.72 W/m·K. The statistical uncertainty ξ is much smaller than ϕ_{nor}, indicating the accuracy of the measurement. Curves with thermal conductivities of 3.42 W/m·K and 4.02 W/m·K demonstrate the fitting uncertainty. (b) The raw data of samples and the calibration amplitude (inset plot). (c) The fitting result based on the amplitude method. The normalized amplitude A_{nor} (black dots, mV) increases against the frequency f. The thermal conductivity is determined at 3.58 W/m·K.

accurately by the amplitude method. We found the fitting result is not sensitive to the interface thermal resistance. $R''_{\mathrm{Si,SiC}} = 1.5 \times 10^{-7}$ m^2·K/W and $R''_{\mathrm{Si,SiC}} = 0$ m^2·K/W give undistinguishable fitting curves when other parameters are fixed. More detailed studies are given in the next section.

D. Raman characterization

Compared with the results from the phase shift method, the amplitude method excellently determines the thermal conductivity of the film. The thermal conductivity of the SiC films reported

TABLE I. Thermal conductivity determination based on phase shift and amplitude.

Sample	Description	Thickness	Thermal conductivity k (W/m·K)		$R''_{Si,SiC}$ ($m^2 \cdot K/W$)
			Phase shift	Amplitude	Phase shift
1	$Si_{50}C_{50}$	2.5 μm	3.72	3.58	1.5×10^{-7}
2	$Si_{50}C_{50}$	2.5 μm	3.86	3.59	1.1×10^{-7}
3	$Si_{20}C_{80}$	3.5 μm	2.21	2.59	1.5×10^{-7}
4	SiO_2	500 nm	1.31	1.68	$<10^{-8}$

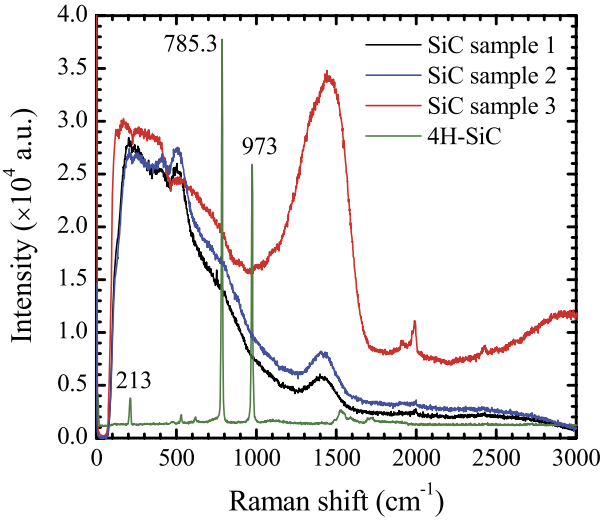

FIG. 3. Raman spectra of the SiC samples and bulk 4H-SiC single crystal under the same measurement condition. The bulk SiC single crystal shows clear sharp peaks indicating good crystalline structures, while the CVD SiC samples only have broad peaks demonstrating their amorphous structures.

in Table I is obviously lower than that of bulk SiC: from 360 W/m·K to higher.[26] This significant reduction in thermal conductivity is mainly attributed to structures of CVD SiC. To study the internal structure of those films, a confocal Raman spectrometer (Voyage, B&W Tek, Inc.) installed with a 532 nm excitation laser and a microscope (Olympus BX51) are used for structure characterization. The Raman laser beam is focused by using a 50× microscope objective, with a focal point size of about 8 μm^2. The resolution of this Raman spectrum is 1.05-1.99 cm^{-1}. All samples are characterized and spectra are all recorded at room temperature (20 °C) in the open air.

The clear differences between samples 1, 2, 3, and the crystal 4H-SiC are shown in the Raman spectra in Fig. 3. For the 4H-SiC crystal, its Raman spectrum has several sharp peaks at 212 cm^{-1} (FTA mode for 4H polytype), 785 cm^{-1} (TO band) and 973 cm^{-1} (LO band).[27,28] However, for our CVD SiC films, only several broad peaks are observed. Samples 1 and 2 have the same composition of Si and C in the SiC film, so their Raman spectra are almost the same and have a small broad peak at 1410 cm^{-1}. Due to its different ratio of Si and C from sample 1 and 2, sample 3 shows a slightly different spectrum. It also has the broad 1410 cm^{-1} peak, but the peak is much stronger than that of samples 1 and 2. The 1410 cm^{-1} peak is associated with stretching vibration mode of the C-C bond,[29] which indicates the formation of carbon clusters in all three CVD SiC films. Sample 3 has a high concentration of C than sample 1 and 2. A large amount of C may form homonuclear C-C bond in the carbon clusters instead of forming Si-C bonds. The weak peak around 500 cm^{-1} indicates some silicon clusters in the films. According to the Raman spectra, the crystal SiC has several sharp peaks showing high crystallinity, while the CVD samples have only a broad and weak peak around

700 cm^{-1} for Si-C bond (shown as a shoulder in Fig. 3) indicating low concentration and small grain size of SiC crystals within the film and other amorphous structures.

Since the single crystalline 4H-SiC is a long range ordered crystal, its optical phonons are largely restricted to one scattering mode and produce a narrow peak. However, the nanocrystalline SiC optically allows more phonon scattering modes to broaden peaks due to its smaller grain size.[30] The SiC films measured here are grown on a Si substrate. Lattice mismatch at the SiC/Si interface will occur at the beginning of growth, leading to significantly reduced crystallinity of the film. Additionally, if the growth is not epitaxial, nanograins will exist in the film. Such small size grains will significantly enhance phonon scattering mainly at the grain boundary, and broaden the Raman peak. The grain boundary-induced phonon scattering also could change the phonon dispersion relation, leading to further thermal conductivity reduction. As a result, a substantially reduced thermal conductivity is expected. Moreover, sample 3 contains more carbon clusters than sample 1 and 2 due to the strong 1410 cm^{-1} peak in sample 3's Raman spectrum. The low thermal conductivity of amorphous structures in carbon clusters further lowers the overall thermal conductivity of sample 3.

E. Thermal transport across 500 nm thick SiO_2 film

For the purpose of comparison and studying the accuracy of the amplitude method, we also measure another sample (Sample 4) that is composed of a thin layer of SiO_2 on a Si substrate. The SiO_2 layer is grown via thermal oxidation and has a thickness of 500 nm. A 60 nm Ir coating covers the top of SiO_2 layer and performs the same function as the Cr film for SiC samples. The Ir coating has a thermal conductivity of 147 W/m·K, density of 2.256×10^4 kg/m^3, and specific heat of 131 J/kg·K. For the SiO_2 film, density (2200 kg/m^3) and specific heat (745 J/kg·K) of bulk SiO_2 are used here for the 500 nm thermal oxidation layer during data processing.

The fitted curves for both phase shift and amplitude methods are plotted in Fig. 4 and fitted thermal conductivities are listed in Table I. The best fitted thermal conductivity of SiO_2 is 1.31 W/m·K based on the phase shift method. The corresponding interfacial thermal resistance is less than 10^{-8} m^2·K/W, which is too small to be determined accurately. The k from the phase shift method is very close to the reference bulk's value (1.38 W/m·K). For the amplitude fitting method, k of SiO_2 is determined to be 1.68±0.17 W/m·K and R''_{Si,SiO_2} is also less than 10^{-8} m^2·K/W. This

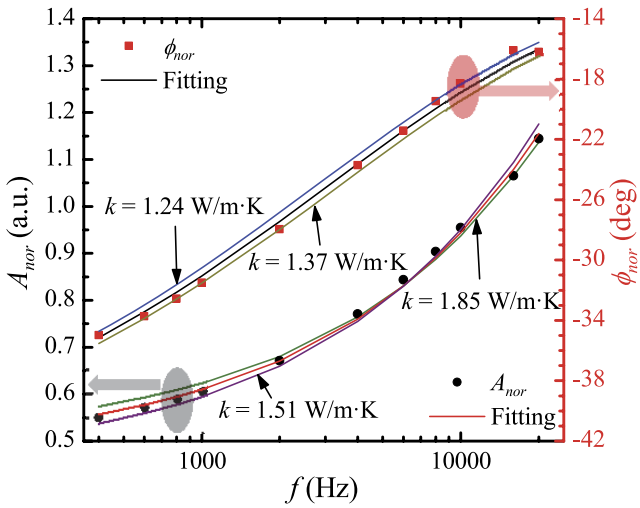

FIG. 4. Fitting results based on the phase shift and the amplitude methods for the 500 nm thick SiO_2 film on Si. With the phase shift method, the thermal conductivity is determined to be 1.31 W/m·K. Theoretical curves with thermal conductivities of 1.24 W/m·K and 1.37 W/m·K demonstrate the fitting uncertainty. With the amplitude method, the thermal conductivity is determined to be 1.68 W/m·K. The fitting uncertainty is illustrated with curves of thermal conductivities of 1.51 W/m·K and 1.85 W/m·K.

k is 24% higher than that from the phase shift method or the value in literature. The thin thickness of SiO_2 is one reason that causes this deviation and gives large uncertainty. Usually when the film is very thin, its own thermal resistance L/k (thermal resistance per unit area) is very small. For the SiO_2 layer (500 nm), L/k is about 3.8×10^{-7} m^2·K/W. Its effect on the phase shift and amplitude becomes weak. In the experiment, the small variation in normalized amplitude will lower the sensitivity of k in the fitting process. In Fig. 4, the percentage of the increment of A_{nor} in SiO_2/Si sample is smaller than that in SiC/Si sample. More thermal energy penetrates into the substrate and the effusivity of Si strongly affects the amplitude of thermal radiation which is detailed in the next section. If a pure bulk sample is measured by using the amplitude method, the normalized amplitude variation would be 0 (flat A_{nor} against frequency).

IV. SENSITIVITY STUDY OF PARAMETERS

A. Sensitivity study of thermal contact resistance

As mentioned above, the interface resistance cannot be precisely determined in the amplitude fitting even though it is very sensitive to the film's thermal conductivity. In the theoretical calculation, the role of the interface resistance is illustrated in Eq. (4a). The term $k_{i+1}\sigma_{i+1}/k_i\sigma_i$ can be simplified to e_{i+1}/e_i, where e_i is the effusivity of the layer i. It is the ratio of effusivity e between the sample layer and the substrate. In our case study, the interaction between SiC layer and Si substrate dominates the thermal transport through the whole sample. Therefore, the term $k_{i+1}\sigma_{i+1}/k_i\sigma_i$ can be expressed as e_{SiC}/e_{Si}, which is the effusivity ratio of SiC layer to Si substrate. This ratio is usually smaller than 1 depending on how the sample is designed and is calculated to be around 0.03 with the fitting result for our samples.

$k_{i+1}\sigma_{i+1}R_{i,i+1}$ is the only term relevant to the interfacial thermal contact resistance in the theoretical calculation. It can be deduced as $(1+j)\sqrt{\pi f}\cdot e_{i+1}\cdot R_{i,i+1}$, in which f is the only variable in the PT measurement. $R_{i,i+1}$ is $R''_{Si,SiC}$ in the present work. Clearly, the effect of $R_{i,i+1}$ is mainly dependent upon the frequency. Furthermore, the SiC is grown on the Si surface by using the CVD method, thus the connection between these two layers should be good. $R_{i,i+1}$ will be small, around 10^{-7} m^2·K/W according to our fitting result. For a very high frequency, the resistance effect becomes more important and contributes to the total value of Eq. (4a). For example, the value of this term reaches 10^{-2} at a frequency of 10 kHz. Compared with the terms "1" and $k_{i+1}\sigma_{i+1}/k_i\sigma_i$, $(1+j)\sqrt{\pi f}\cdot e_{i+1}\cdot R_{i,i+1}$ is much smaller, especially in the low frequency range in Eq. (4a). However, in the phase shift method, phase shift changes more relative to amplitude with the same variation of $R_{i,i+1}$. Therefore, the phase shift method is more sensitive to the interfacial resistance. For the exponent term $\exp[\mp\sigma_{i+1}(l_{i+1}-l_i)]$, its value is determined by the thickness of the sample layer. Samples measured by the PT technique in our case have a thickness of several micrometers or fewer, so the value of this term is approximately equal to 1.

A study of $R''_{Si,SiC}$ is therefore conducted for sample 1 to reveal the sensitivity of the thermal contact resistance in the amplitude method. The residual (r) of the least square calculation determines the quality of the resulting curve in the fitting process. It is defined as the standard deviation of $(A_{nor,exp} - C\cdot A_{nor,the})$ at all recorded frequencies. The relationship between r and the thermal resistance $R''_{Si,SiC}$ is plotted in Fig. 5(a). The residual r clearly begins to increase when $R''_{Si,SiC}$ is larger than 10^{-7} m^2·K/W. However, the interface of the CVD SiC film on the Si substrate should have a good contact so that $R''_{Si,SiC}$ should not be larger than 10^{-6} m^2·K/W. Thus, the thermal contact resistance is not sensitive in our case.

B. Importance of effusivity

From the physical model described in Sec. II, the interfacial transmission matrix of heat and then $k_i\sigma_i$ and $\sigma_i L_i$ in Eq. (4a) for each layer in the sample are obtained directly and independently. Thus, in the fitting process, $k\rho c_p$ (thermal effusivity) and L/k (thermal resistance per unit area) can be determined with high accuracy and will not be affected by the uncertainty of thickness measurement. For individual thermal parameters, k and ρc_p, further calculation are need and will give rise

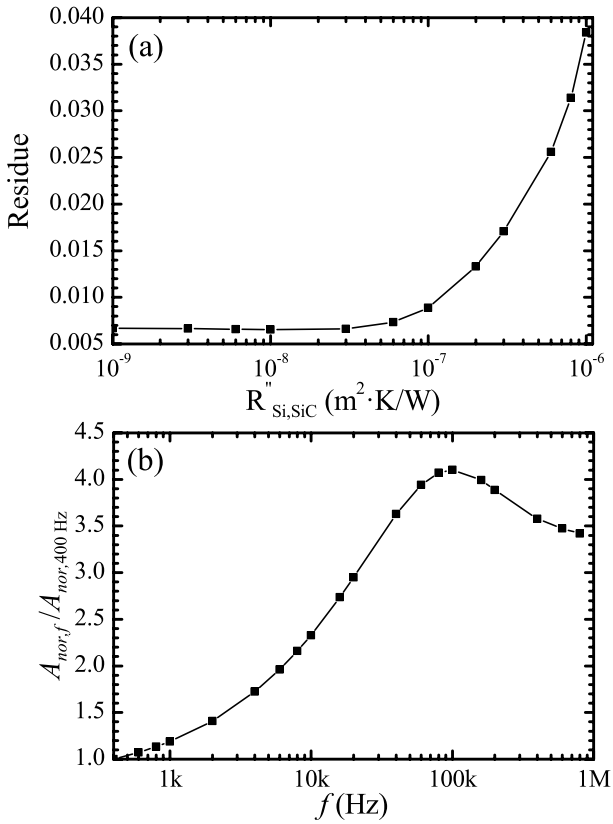

FIG. 5. (a) Residual of the least square method against the thermal contact resistance $R''_{Si,SiC}$ for sample 1. The residual does not change much against $R''_{Si,SiC}$ until it is larger than 10^{-7} m^2·K/W, so the amplitude method is not sensitive to $R''_{Si,SiC}$. (b) The ratio $A_{nor,f}/A_{nor,400\ Hz}$ against the frequency with all parameters from sample 1. The rest parameters for sample 1 are fixed for these two plots: k is 3.58 W/m·K, ρ is 3160 kg/m^3, c_p is 690 J/kg·K, and d is 2.5 μm, and $R''_{Si,SiC}$ is 1.51×10^{-7} m^2·K/W for Fig. 4(b).

to their experimental uncertainty. The thermal effusivity is an important and reliable parameter for evaluating the amplitude method.

In the amplitude method, the normalized amplitude A_{nor} directly shows the effect of thermal diffusion length changing against an increasing frequency. The thermal diffusion length is proportional to $1/\sqrt{f}$. The thermal radiation signal will be affected by the thermophysical properties of the sample layer and the substrate at a low moderated frequency, while the sample layer's property contributes primarily to the radiation signal at a high frequency. Based on this analysis, a simple assessment of the accuracy of the amplitude method can be conducted directly from A_{nor}.

The ratio $A_{nor,f}/A_{nor,400\ Hz}$ is thereby introduced to study the accuracy of the amplitude normalization and the amplitude method. This relationship between $A_{nor,f}/A_{nor,400\ Hz}$ and the frequency is shown in Fig. 5(b) with fixed parameters from sample 1: density ρ = 3160 kg/m^3, thermal conductivity k = 3.58 W/m·K, specific heat c_p = 690 J/kg·K, and the thickness of the film L = 2.5 μm. The calculation of the curve starts at 400 Hz to guarantee the assumption of the 1D model. Also, 400 Hz is the same as the start frequency in the experiment. The frequency ends at 0.9 MHz, which is much larger than 20 kHz in the experiment. The theoretical calculation to this high frequency is for exploring the effect of the Cr layer on the thermal radiation signals, though such high frequency is unnecessary in the experiment. Figure 5(b) shows a gradual increase for the curve against the modulated frequency when the frequency is lower than 100 kHz. After rising to a maximum of 100 kHz, the amplitude ratio begins to decrease.

According to the expression of thermal diffusion length $\mu_i = \sqrt{\alpha_i/\pi f}$, the diffusion depth is longer in the low frequency range. $\mu_{SiC,400\ Hz}$ is approximately 36 μm at 400 Hz which is longer

than the thickness of the SiC film (2.5 μm). The thermal energy can pass through the SiC film and significantly penetrating into the Si substrate. The effusivity of Si dominates the effective effusivity of the sample. When the frequency rises to 100 kHz, $\mu_{\mathrm{SiC,100\ kHz}}$ becomes 2.29 μm. The thermal energy is only transferred inside the SiC film and the radiation signal is mainly related to the SiC properties. The data point at 100 kHz in Fig. 5(b) is selected for further discussion. The theoretical fitted value of the ratio $A_{nor,100\ \mathrm{kHz}}/A_{nor,400\ \mathrm{Hz}}$ is 4.10 in the experiment. In contrast, it has $A_{nor,100\ \mathrm{kHz}}/A_{nor,400\ \mathrm{Hz}} \approx \sqrt{(k\rho c_p)_{\mathrm{Si}}/(k\rho c_p)_{\mathrm{SiC}}} = 5.60$ based on Eq. (7), which is slightly larger than the theoretical fitted ratio. $A_{nor,400\ \mathrm{Hz}}$ is a combined result of both SiC and Si effects at the low frequency of 400 Hz because both SiC and Si contribute portions of the amplitude of the total thermal radiation from the Cr surface. Since e_{SiC} (2.85×10^3 W/m^2·K·s$^{0.5}$) is lower e_{Si} (1.57×10^4 W/m^2·K·s$^{0.5}$), this combination lowers $\sqrt{(k\rho c_p)}$ at 400 Hz. The effect of Cr is negligible at 400 Hz.

At the frequency of 100 kHz, the thermal diffusion length in SiC becomes shorter (2.29 μm) than the SiC film's thickness, and thus the Si substrate has negligible effect on the thermal radiation. In contrast, the Cr film plays an important role in determining the effective effusivity. Since the effusivity of Cr (1.74×10^4 W/m^2·K·s$^{0.5}$) is much higher than that of SiC (2.85×10^3 W/m^2·K·s$^{0.5}$), e_{Cr} increases e_{eff} that determines the thermal radiation signal. Both of these two factors cause the deviation in the amplitude ratio between our theoretical fitting and the real effusivity. When the frequency is higher than 100 kHz, the normalized amplitude ratio gradually decays compared with the ratio at 100 kHz in Fig. 5(b). The reduction results from the increasing effect of the Cr film. At frequencies higher than 100 kHz, the SiC's thermophysical property contributes less to the thermal radiation because the thickness of the SiC film continues decreasing. The effective effusivity to determine the amplitude is a combined effect of e_{Cr} and e_{SiC}. e_{eff} is increased due to the decreasing portion of e_{SiC} when the frequency continues to increase. The normalized amplitude ratio $A_{nor,>100\ \mathrm{kHz}}/A_{nor,400\ \mathrm{Hz}} = \sqrt{(k\rho c_p)_{\mathrm{Si}}/(k\rho c_p)_{eff}}$ thereby decreases against the frequency increment. It is easily understood that the amplitude of thermal radiation is a constant for a pure bulk material because of the constant effusivity. Nevertheless, the ratio of the normalized amplitude at sufficiently high frequencies to that at low frequencies can be used as a quick indicator to evaluate the effusivity ratio of the film to the substrate.

The amplitude method has the characteristic that the interface resistance is less sensitive. It can thereby help determine the thermal conductivity of the film accurately with little effect from the interface resistance. Moreover, the ratio of normalized amplitude provides a good way to directly evaluate the effusivity of the sample film.

V. CONCLUSION

In this work, an amplitude method for the PT technique has been developed to analyze the thermal radiation signal from the surface of a multilayered sample. There CVD SiC film samples and a SiO_2 film sample on a silicon substrate were characterized using the amplitude method. The determined thermal conductivity based on the amplitude method is 3.58, 3.59, and 2.59 W/m·K for SiC sample 1 to 3, respectively. The accuracy of the amplitude method was verified by comparing it with the reliable phase shift method. The resulting thermal conductivity of all SiC samples from the two methods agreed well with each other. For the SiO_2 film on Si substrate, the thermal conductivity is measured to be 1.68 W/m·K which is a little higher than that determined by the phase shift method: 1.31 W/m·K. The normalized amplitude (A_{nor}) defined in our amplitude method is closely related to the effusivity of the film and substrate. The ratio of A_{nor} at a sufficiently high frequency to that at a low frequency provides a sound estimate of the effusivity ratio of the film to the substrate. In addition, the non-sensitive nature of thermal contact resistance in the amplitude method was observed through studying the sensitivity of parameters. The reason for weak sensitivity has been specifically discussed with the expression and physical meanings of interfacial transmission matrix. However, this feature allows for the amplitude method to fit the thermal conductivity of samples with little effect from the interfacial resistance in multilayered samples, and provides a reliable alternative to study the thermophysical properties of films in the thickness direction.

ACKNOWLEDGMENTS

Support of this work by the Army Research Office (W911NF-12-1-0272), Office of Naval Research (N000141210603), and National Science Foundation (CBET-1235852) is gratefully acknowledged. XW thanks the partial support of "Taishan Scholar" program of Shandong Province, China.

[1] L. Lu, W. Yi, and D. L. Zhang, Rev. Sci. Instrum. **72**, 2996 (2001).
[2] T. Y. Choi, D. Poulikakos, J. Tharian, and U. Sennhauser, Appl. Phys. Lett. **87**, 013108 (2005).
[3] T. Y. Choi, D. Poulikakos, J. Tharian, and U. Sennhauser, Nano Lett. **6**, 1589 (2006).
[4] S. Sporlein, H. Carstens, H. Satzger, C. Renner, R. Behrendt, L. Moroder, P. Tavan, W. Zinth, and J. Wachtveitl, Proc. Natl. Acad. Sci. U. S. A. **99**, 7998 (2002).
[5] O. J. Korovyanko, C. X. Sheng, Z. V. Vardeny, A. B. Dalton, and R. H. Baughman, Phys. Rev. Lett. **92**, 017403 (2004).
[6] C. Thomsen, H. T. Grahn, H. J. Maris, and J. Tauc, Phys. Rev. B **34**, 4129 (1986).
[7] M. Ducousso, T. Dehoux, C. Rossignol, B. Audoin, O. Zouani, C. Chollet, C. Chanseau, and M. C. Durrieu, J. Phys.: Conf. Ser. **278**, 012042 (2011).
[8] R. Anastasi, *Ultrasonic and Advanced Methods for Nondestructive Testing and Material Characterization* (World Scientific Publishing, 2007).
[9] C. A. Paddock and G. L. Eesley, J. Appl. Phys. **60**, 285 (1986).
[10] K. Ujihara, J. Appl. Phys. **43**, 2376 (1972).
[11] G. L. Eesley, Ieee J. Quantum Electron. **17**, 1285 (1981).
[12] A. Rosencwaig and A. Gersho, J. Appl. Phys. **47**, 64 (1976).
[13] S. D. Campbell, S. S. Yee, and M. A. Afromowitz, IEEE Trans. Biomed. Eng. **26**, 220 (1979).
[14] N. C. Fernelius, J. Appl. Phys. **51**, 650 (1980).
[15] T. Fujii, K. Kumosaki, and M. Inoue, J. Appl. Phys. **52**, 2350 (1981).
[16] J. Baumann and R. Tilgner, J. Appl. Phys. **58**, 1982 (1985).
[17] H. P. Hu, X. W. Wang, and X. F. Xu, J. Appl. Phys. **86**, 3953 (1999).
[18] X. W. Wang, Z. R. Zhong, and J. Xu, J. Appl. Phys. **97**, 064302 (2005).
[19] T. Wang, X. W. Wang, Y. W. Zhang, L. Y. Liu, L. Xu, Y. Liu, L. J. Zhang, Z. Y. Luo, and K. F. Cen, J. Appl. Phys. **104**, 013528 (2008).
[20] X. W. Chen, Y. P. He, Y. P. Zhao, and X. W. Wang, Nanotechnology **21**, 055707 (2010).
[21] J. Q. Guo, X. W. Wang, D. B. Geohegan, and G. Eres, Funct. Mater. Lett. **1**, 71 (2008).
[22] J. Q. Guo, X. W. Wang, D. B. Geohegan, G. Eres, and C. Vincent, J. Appl. Phys. **103**, 113505 (2008).
[23] X. H. Feng, G. Q. Liu, S. Xu, H. Lin, and X. W. Wang, Polymer **54**, 1887 (2013).
[24] C. A. Bennett and R. R. Patty, Appl. Opt. **21**, 49 (1982).
[25] D. R. Lide, *CRC Handbook of Chemistry and Physics* (Taylor and Francis, Boca Raton, FL, 2007).
[26] G. Yu, L. M.E., and R. S.L., *Properties of Advanced Semiconductor Materials GaN, AlN, SiC, BN, SiC, SiGe* (John Wiley & Sons, Inc., New York, 2001).
[27] S. Nakashima and H. Harima, Phys. Status Solidi A **162**, 39 (1997).
[28] D. W. Feldman, J. H. Parker, W. J. Choyke, and L. Patrick, Phys. Rev. **173**, 787 (1968).
[29] P. Musumeci, F. Roccaforte, and R. Reitano, Europhys Lett. **55**, 674 (2001).
[30] S. Xu, X. D. Tang, Y. N. Yue, and X. W. Wang, J. Raman Spectrosc. **44**, 1523 (2013).